THE JOURNAL OF BIOLOGICAL CHEMISTRY VOL. 289, NO. 49, pp. 33862–33873, December 5, 2014

Cardiac Function Is Regulated by B56α-mediated Targeting of Protein Phosphatase 2A (PP2A) to Contractile Relevant Substrates*

Received for publication, July 22, 2014, and in revised form, October 2, 2014 Published, JBC Papers in Press, October 15, 2014, DOI 10.1074/jbc.M114.598938

Uwe Kirchhefer[‡1], Christiane Brekle[‡], John Eskandar[‡], Gunnar Isensee[‡], Dana Kučerová[‡], Frank U. Müller[‡], Florence Pinet[§], Jan S. Schulte[‡], Matthias D. Seidl[‡], and Peter Boknik[‡]

From the [‡]Institut für Pharmakologie und Toxikologie, Universitätsklinikum Münster, D-48149 Münster, Germany and [§]INSERM, U744, Institut Pasteur de Lille, 59019 Lille, France

Background: PP2A is a regulator of cardiac excitation-contraction coupling.
Results: Cardiomyocyte-directed overexpression of B56α, the main cardiac PP2A regulatory subunit, results in the dephosphorylation of myofilament proteins, increased Ca^{2+} sensitivity, and higher contractility.
Conclusion: This suggests an important role for B56α in regulating PP2A activity and thereby the contractile function.
Significance: PP2A-B56α is a potential pharmacological target to improve cardiac performance in failing hearts.

Dephosphorylation of important myocardial proteins is regulated by protein phosphatase 2A (PP2A), representing a heterotrimer that is comprised of catalytic, scaffolding, and regulatory (B) subunits. There is a multitude of B subunit family members directing the PP2A holoenzyme to different myocellular compartments. To gain a better understanding of how these B subunits contribute to the regulation of cardiac performance, we generated transgenic (TG) mice with cardiomyocyte-directed overexpression of B56α, a phosphoprotein of the PP2A-B56 family. The 2-fold overexpression of B56α was associated with an enhanced PP2A activity that was localized mainly in the cytoplasm and myofilament fraction. Contractility was enhanced both at the whole heart level and in isolated cardiomyocytes of TG compared with WT mice. However, peak amplitude of $[Ca]_i$ did not differ between TG and WT cardiomyocytes. The basal phosphorylation of cardiac troponin inhibitor (cTnI) and the myosin-binding protein C was reduced by 26 and 35%, respectively, in TG compared with WT hearts. The stimulation of β-adrenergic receptors by isoproterenol (ISO) resulted in an impaired contractile response of TG hearts. At a depolarizing potential of −5 mV, the $I_{Ca,L}$ current density was decreased by 28% after administration of ISO in TG cardiomyocytes. In addition, the ISO-stimulated phosphorylation of phospholamban at Ser^{16} was reduced by 27% in TG hearts. Thus, the increased PP2A-B56α activity in TG hearts is localized to specific subcellular sites leading to the dephosphorylation of important contractile proteins. This may result in higher myofilament Ca^{2+} sensitivity and increased basal contractility in TG hearts. These effects were reversed by β-adrenergic stimulation.

Phosphorylation and dephosphorylation are two opposite processes that control excitation-contraction coupling in cardiomyocytes. One of the main serine/threonine phosphatase activities is due to protein phosphatase 2A (PP2A).[2] In the heart, PP2A function is linked to the regulation of β-adrenergic signaling, sarcoplasmic reticulum (SR) Ca^{2+} handling, contractility/relaxation, and the modulation of ion channel activities. In detail, PP2A is thought to be the cardiac phosphatase mainly responsible for dephosphorylating cTnI, phospholamban, the ryanodine receptor, and the L-type Ca^{2+} channel (1–3). The importance of PP2A in maintaining normal cardiac function has also been demonstrated in studies using the purified catalytic subunit in isolated cardiomyocytes (4), specific phosphatase inhibitors like okadaic acid or cantharidin (5, 6), and transgenic expression models (7). The current challenge is to understand how the diversity of PP2A subunit composition contributes to the targeting of the enzyme activity to specific substrates in defined myocellular compartments.

PP2A enzymes are heterodimeric complexes consisting of a conserved catalytic subunit ($PP2A_C$) and a scaffolding subunit ($PP2A_A$). There are 13 known PP2A regulatory B subunits that target the phosphatase activity to various cellular compartments or organelles, confer substrate specificity, or control enzyme activity (8). The B subunits are grouped into four unrelated gene families termed B (B55), B′ (B56), B″, and B‴ (9). On the other hand, B56 is the most diverse gene family of B subunits, consisting of five isoforms that are differentially expressed in many tissues and cell types (10). B56α exhibits the highest expression in the heart and skeletal muscle (10, 11). It has been demonstrated that B56α is a phosphoprotein like most of the B56 family members (12). We have recently shown that nonphosphorylated B56α inhibited purified $PP2A_{CA}$ activity (13). The potency of B56α for PP2A inhibition was markedly increased by a phosphorylation of B56α at Ser^{41} by PKC.

* This work was supported by Innovative Medizinische Forschung Münster Grant KI 2 1 10 10.
[1] To whom correspondence should be addressed: Inst. für Pharmakologie und Toxikologie, Universitätsklinikum Münster, Domagkstr. 12, D-48149 Münster, Germany. Tel.: 49-251-8352606; E-mail: kirchhef@uni-muenster.de.

[2] The abbreviations used are: PP2A, protein phosphatase 2A; PP, protein phosphatase; SR, sarcoplasmic reticulum; ISO, isoproterenol; TG, transgenic; LV, left ventricular; SL, sarcomere length; PLN, phospholamban; TnI, troponin inhibitor; MyBP-C, myosin-binding protein C; MLC-2, myosin light chain 2; cTnI, cardiac troponin inhibitor; TnT, troponin T.

B56α binds to regulatory proteins via an ancillary adapter protein, ankyrin B (14). This directs different PP2A species to distinct subcellular locales in cardiomyocytes. Deletion of ankyrin B resulted in a disorganized distribution of B56α in the heart (14). After adenovirus-mediated transfection of neonatal rat cardiomyocytes, B56α displayed a meshwork cytoplasmic distribution, frequently with a striated pattern (*i.e.* co-localized with the myofilaments), but was excluded from the nucleus (15). Analysis of myocardial fractions revealed that B56α was decreased in the myofilament fraction and increased in the cytosol after β-adrenergic stimulation by isoproterenol (ISO) (16). These dynamic changes in PP2A-B56α targeting may contribute to neurohumoral regulation of cardiac performance under physiological conditions and in the diseased heart, as demonstrated for sepsis-associated cardiac dysfunction (17).

Based on these findings, we hypothesized that a higher expression of B56α in the heart might favor proper targeting of PP2A to specific subcellular domains, leading to a sustained dephosphorylation of myofilament proteins, which then alters cardiac contractility. For this purpose, we generated transgenic mice with cardiomyocyte-directed overexpression of B56α and characterized the effects on PP2A regulation and cardiac function.

EXPERIMENTAL PROCEDURES

Materials—[γ-^{32}P] ATP was obtained from Hartmann Analytic. All other chemicals were of reagent grade.

B56α-overexpressing Mice—B56α cDNA was generated as recently described (13). The amplified cDNA fragment contained engineered SalI restriction enzyme sites at both ends. This B56α cDNA fragment was subcloned into a mouse cardiac α-myosin heavy chain promoter expression cassette (18). The orientation of the B56α cDNA was confirmed by sequencing (GATC). Generation of transgenic mice and screening were performed by standard procedures. Ten B56α transgenic mouse founders were obtained. Two of them were crossed with DBA/C3H mice for propagation and generation of experimental animals. Experiments were performed on mice 14–18 weeks of age. Animals were handled and maintained according to protocols approved by the animal welfare committee of the University of Münster, which also conform to the National Institutes of Health Guidelines for the Care and Use of Laboratory Animals.

Immunohistochemistry and Fibrosis Staining—Cross-sections from the left ventricular (LV) wall were fixed with 4% buffered paraformaldehyde, dehydrated with graded concentrations of isopropyl alcohol, embedded in paraffin, and cut into 5-μm slices. Only areas with transversely cut muscle fibers were used for stainings. Sections were treated with affinity-purified polyclonal antibodies raised against either B56α (recognizing both the endogenous mouse and the transgenic human B56α; Bethyl) or the catalytic subunit of PP2A (Proteintech Group) followed by incubation with the ImmPRESS reagent (Vector Laboratories). Visualization was enabled by application of chromogenic peroxidase substrates VIP (B56α) or diaminobenzidine (Cα). This procedure resulted in a purple- or brown-colored precipitate at the B56α or Cα location, respectively. Sections were counterstained with hematoxylin and mounted with coverslips. Masson-Goldner staining was used to detect fibrosis.

Immunofluorescence Stainings—Isolated cardiomyocytes were incubated for 15 min on polylysine-coated slides, and the attached cells were fixed by a 5-min incubation with methanol and washed with PBS. After applying a cover slide, the cells were frozen, followed by a freeze-crack by removing the cover slide with a scalpel.

The cells were incubated in 0.1% goat serum (Sigma-Aldrich) in PBS-T (PBS with 1% Tween 20) blocking solution for 50 min, followed by a 1-h treatment with an antibody directed against human B56α (1:200; Bethyl) in blocking solution. After washing (generally 3 × 10 min in PBS), cardiomyocytes were incubated for 1 h at room temperature with secondary antibody Alexa Fluor 488 (Alexa Fluor® 488 chicken anti-rabbit IgG, 1:500; Invitrogen). After washing the cells were blocked with unconjugated Fab fragments (goat anti-mouse IgG (H+L) unconjugated; Dianova) for 1 h. Thereafter, an antibody directed against $PP2A_C$ (1:200; BD Transduction Laboratories) was applied for 1 h, followed by washing and an incubation with secondary antibody Alexa Fluor 594 (Alexa Fluor® 594 goat anti-mouse IgG, 1:500; Invitrogen) for 1 h at room temperature. The nuclei were stained by DAPI (10 pg/ml in distilled water). Fluorescence was detected by use of a fluorescence microscope (Ti-E Eclipse; Nikon) or a confocal laser scanning microscope (LSM 710; Carl Zeiss AG).

Preparation of Cardiac Subcellular Fractions—Subcellular fractions (cytosol, myofilaments, and membranes) were prepared from whole heart homogenates as described (19). This protocol allows the preparation of cardiomyocyte-derived fractions enriched in different cellular organelles. The supernatant obtained after the first centrifugation of heart homogenates was named cytosol. It can be suggested that most of the fibroblasts, constituting the main fraction of noncardiomyocyte cells, are enriched in the pellet after the first centrifugation. Thus, the cytosol fraction should contain mostly proteins derived from cardiomyocytes. Moreover, this preparation protocol enables the preparation of purified cardiac myofibrils that are virtually free of contamination by mitochondrial, sarcolemmal, and sarcoplasmic reticulum membranes (20). The membrane-enriched fraction, obtained from this protocol, contains sarcolemmal as well as SR proteins. However, it cannot be excluded that fractions contain small quantities of noncardiomyocyte cells.

Protein Phosphatase Assay—Protein phosphatase activity was assayed using [^{32}P]phosphorylase *a* as substrate as previously described (21). Protein phosphatase activity was determined in extracts of ventricular homogenates or isolated cardiomyocytes, as well as in subcellular fractions. Dephosphorylation reactions were initiated by adding [^{32}P]phosphorylase *a* to a final concentration of 0.5 mg/ml (40,000 cpm/nmol) and carried out at 30 °C for 20 min in the absence or presence of 3 nM okadaic acid. No more than 18% of the substrate were utilized in the assay to assure linearity of the reaction.

Langendorff Perfusion and Working Heart—Heart preparations were utilized as described previously (22). Mice were anesthetized intraperitoneally with 2.0 g of urethane/kg of body

weight and treated with 1.5 units of heparin. The hearts were removed from the opened chest, immediately attached by the aorta to a 20-gauge cannula, and perfused retrogradely with oxygenized Krebs-Henseleit buffer (37.4 °C) containing 118 mM NaCl, 25 mM $NaHCO_3$, 0.5 mM Na-EDTA, 4.7 mM KCl, 1.2 mM KH_2PO_4, 1.2 mM $MgSO_4$, 2.5 mM $CaCl_2$, and 11 mM glucose in an isolated heart system (Hugo Sachs Elektronik). For working heart preparation, the pulmonary vein was cannulated during the retrograde perfusion period. The perfusion of the heart was then changed to an anterograde mode. The venous return (preload) and the aortic pressure (afterload) were adjusted to 5 ml/min cardiac output and 50 mm Hg, respectively. Hearts were stimulated at 8 Hz. Heart rate, aortic pressure, and LV pressure were measured and monitored continuously. The first derivative of LV pressure (+dP/dt and −dP/dt) was calculated (ADInstruments).

Isolation of Cardiomyocytes—Ventricular cardiomyocytes of 14–18-week-old animals were isolated by retrograde Langendorff perfusion (22) of the hearts (2.5 ml/min) and by digestion with collagenase (type 2, 200 units/ml; Worthington) and protease (type XIV, 0.33 units/ml; Sigma-Aldrich). Thereafter, the tissue was dispersed in 5 ml of perfusion buffer supplemented with 5% newborn calf serum for sequestration of enzyme activity and incubated for 10 min. After removal of the supernatant, cells were resuspended in 10 ml of perfusion buffer supplied with 5% newborn calf serum, filtered through a nylon gaze, and centrifuged (42 × *g*, 1 min). The cell pellet was transferred to 10 ml of perfusion buffer, wherein the Ca^{2+} concentration was elevated stepwise to 1 mM every 5 min.

Ca^{2+} Transients and Sarcomere Length Shortening—Measurement of cardiomyocyte function was performed using a dual emission photometry system combined with a CCD camera (Myocyte Calcium and Contractility Recording System; IonOptix Ltd.) attached to an epifluorescence microscope (Nikon). Cardiomyocytes were incubated with 23.3 μM Indo-1/AM (Molecular Probes) for 10 min in a chamber mounted on the microscope. This chamber was perfused with bath solution (23), and cardiomyocytes were field-stimulated with 0.5 Hz. The emitted fluorescence was recorded at wavelengths of 405 and 495 nm. The ratio of 405/495 nm was taken as an index of cytosolic Ca^{2+} concentration. The shortening of sarcomere length was detected simultaneously. The maximum contraction was normalized to resting sarcomere length and expressed as a percentage of shortening. Ca^{2+} transients and sarcomere length shortening were also examined under application of 1 μM ISO.

For determining of SR Ca^{2+} load isolated cardiomyocytes were loaded with 4 μM Fluo-4/AM. Cardiomyocytes were perfused with bath solution (23) using a fast solution switching system (Warner Instrument Corp.) and then stimulated at 0.5 Hz. Fluo-4 was excited at 488 nm, and the emitted fluorescence signal was measured at 522 nm. After a 10-s rest period to achieve maximal SR Ca^{2+} load, caffeine-induced Ca^{2+} release was started by rapid application of 10 mM caffeine for 60 s. The F_1/F_0 peak amplitude and the decay kinetics were determined.

L-type Ca^{2+} Channel Currents—Single cardiomyocytes were studied using the perforated patch whole cell patch-clamp technique as described previously (24). Recordings were performed under conditions that suppress Na^+ and K^+ currents. Briefly, Ca^{2+} currents were elicited by voltage steps from a holding potential of −80 mV to increasing test potentials (−40 to +65 mV, Δ5 mV, 400-ms duration) after a 400-ms prepulse to −40 mV to inactivate T-type Ca^{2+} and Na^+ currents. Cell capacitance and I_{Ca} were recorded in the absence or presence of 1 μM ISO with a SEC05-X amplifier (npi electronic, Tamm, Germany).

Immunoblot Analysis—Protein expression analysis was performed on mouse and human ventricular homogenates or subcellular fractions and on immunoprecipitants of mouse heart lysates. Briefly, 50 mg of frozen pulverized mouse or human heart tissue were sonicated at 4 °C for 1 min in a buffer containing 5% SDS, 10 mM $NaHCO_3$, and a protease inhibitor mixture (Roche). Homogenates were centrifuged at 14,000 × *g* for 20 min, and supernatant lysates were subjected to SDS gel electrophoresis. Lysed homogenates or subcellular fractions were mixed with equal volumes of reducing 5% SDS sample buffer and boiled for 5 min before loading. Immunoprecipitants were also solubilized in SDS sample buffer for further processing by gel electrophoresis. For immunoblot analysis of all proteins, 50–200 μg of individual samples were electrophoretically separated on 5 or 10% SDS-polyacrylamide gels (25, 26). Proteins were transferred to nitrocellulose. Thereafter, blots were incubated with specific antibodies raised against the following proteins: B56α of PP2A (amino acids 25–75; Bethyl), Aα of PP2A (Santa Cruz), Cα of PP2A (Proteintech Group), calsequestrin (22), triadin 1 (27), PLN (Badrilla), PLN phospho-Ser^{16} (Badrilla), PLN phospho-Thr^{17} (Badrilla), Cav1.2 phospho-Ser^{1928} (Badrilla), Cav1.2 (Alomone), RyR (28), RyR phospho-Ser^{2808} (Badrilla), TnI (Cell Signaling), TnI phospho-$Ser^{23/24}$ (Cell Signaling), MLC-2 (Alexis), MLC-2 phospho-Ser^{18} (Origene), MyBP-C (LSBio), MyBP-C phospho-Ser^{282} (Enzo), TnT (Proteintech Group), TnT phospho-Ser^{208} (29), and ankyrin B (Santa Cruz). The amounts of bound antibodies were detected by use of secondary antibodies (ECL rabbit/goat IgG, HRP-linked whole antibody; GE Healthcare). Signals were visualized and quantified with the ECL plus detection system (Amersham Biosciences ECL Plus; GE Healthcare) and the ChemiDoc XRS system, respectively.

Quantitative RT-PCR—Total quantification of mRNA levels was performed as described previously with following modifications (24). Briefly, RNA was extracted from isolated cardiomyocytes with the use of TRIzol® (Invitrogen), and 0.5 μg were randomly reversely transcribed to cDNA using the Transcriptor First Strand cDNA synthesis kit (Roche Applied Science). The real time RT-PCR was carried out using a LightCycler 480 system (Roche Applied Science). The PCRs were set up in a 96-well plate in a volume of 20 μl. The reaction components were 2 μl of undiluted cDNA, 10 μl of LightCycler® 480 Sybr Green I Master, 4 μl of H_2O, and 2 μl of each primer (see Table 1; 10 μM). Reactions were incubated at 95 °C for 5 min followed by 45 cycles at 95 °C for 10 s, 60 °C for 15 s, and 72 °C for 20 s. Relative quantification was performed by calculating relative expression ratios using the $\Delta\Delta C_T$ method and the relative expression software tool (REST, version 2.013). Hypoxanthine-guanine phosphoribosyltransferase (*Hprt*) was used as a reference gene.

PKA Activity—PKA activity was determined as previously described (30). Frozen tissue powder was thawed and homogenized for 6 × 10 s at 4 °C in the following buffer: 4 mM EDTA, 15 mM β-mercaptoethanol, pH 7.4. The homogenate was centrifuged for 20 min at 14,000 × *g*. An aliquot of the supernatant was added to an assay mixture (±2 μM cAMP) that contained 30 mM potassium phosphate buffer (pH 6.8), 8.3 mg/ml kemptide, 10 mM $MgCl_2$, 5 mM aminophylline, 0.5 mM ATP, and 5 μCi [γ-^{32}P]ATP. Incubation was performed at 30 °C for 10 min. The reaction was stopped by the addition of 0.2 M EDTA. An aliquot was spotted on P81 phosphocellulose papers (Whatman) that were washed three times with 75 mM phosphoric acid. Filters were dried, and radioactivity was determined in a liquid scintillation counter. PKA activity is expressed as incorporation of pmol of ^{32}P per min and per mg protein.

Statistical Analysis—Statistical differences between groups were calculated by analysis of variance or Kruskal-Wallis one-way analysis of variance on ranks followed by Bonferroni's or Dunn's post hoc tests, respectively. $p < 0.05$ was considered significant.

RESULTS

Overexpression of B56α Results in Higher PP2A Activity—To characterize the role of B56α in regulating cardiac contractility, we generated transgenic mice with cardiomyocyte-directed overexpression of human B56α. Ten transgenic founders were identified. Two of them were cross-bred for propagation and generation of experimental animals. Finally, one lineage was used for biochemical and physiological characterization. Overexpression of B56α was not associated with overt developmental or morphological defects in transgenic mice. The heart and body weights were comparable between TG and WT mice (data not shown). Transgenic mice exhibited a normal life span. The level of B56α expression was assessed in ventricular homogenates by SDS-PAGE followed by immunoblotting (Fig. 1*A*). The antibody was directed against human full-length B56α. Therefore, we used ventricular homogenates of nonfailing human heart as a control sample. The expression of total B56α (including exogenous transgenic human and endogenous mouse B56α) was ~2-fold higher in TG compared with WT hearts (Fig. 1*A*). Because in mouse samples as well as in human nonfailing hearts we detected a second band running at lower molecular mass than the expected mobility form of the protein, immunoprecipitations were performed on wild-type mouse heart lysates (Fig. 1*A*). The identity of B56α was verified by use of a blocking peptide resulting in the disappearance of the specific band of interest (*i.e.* the band just below B56α is nonspecific (Fig. 1*A*). Overexpression of B56α was associated with a ~2-fold higher protein expression of the catalytic subunit of PP2A, whereas the PP1 expression remained unchanged between TG and WT (Fig. 1*A*). To test whether the increased PP2A expression is paralleled by appropriate changes in the enzyme activity, we measured phosphorylase phosphatase activity in supernatants of ventricular homogenates. Total phosphorylase phosphatase activity was enhanced by 24% in TG compared with WT hearts (Fig. 1*B*). To dissect the relative contribution of the activities of PP1 and PP2A, phosphatase activity was also assayed in the presence of 3 nM okadaic acid,

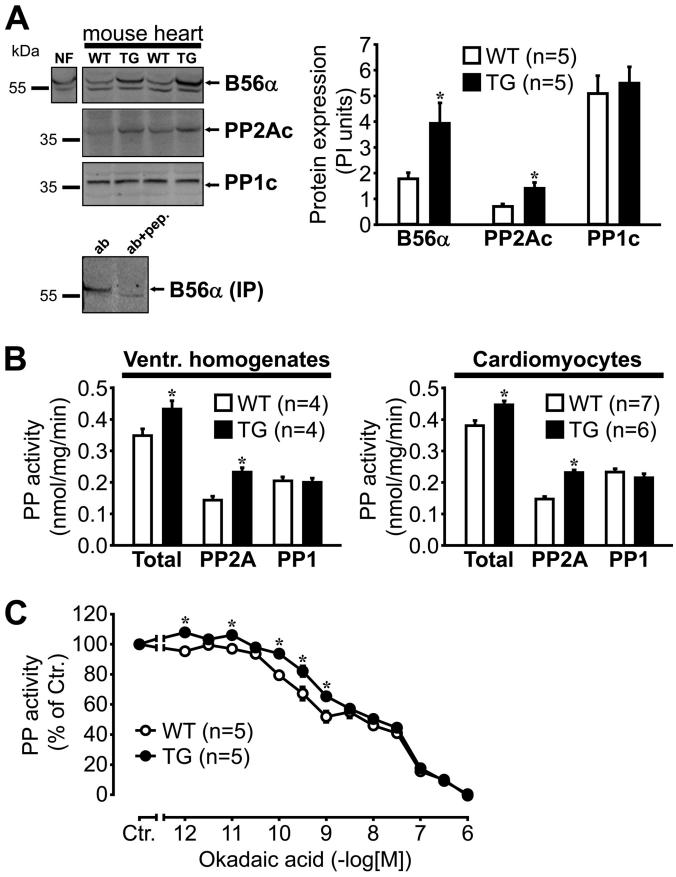

FIGURE 1. **Detection of protein phosphatase subunits and analysis of PP2A activity.** *A*, ventricular tissue of nonfailing human heart (*NF*), as well as of WT and B56α-overexpressing TG mice was homogenized and then subjected to gel electrophoresis and subsequent immunoblotting (*left panel*). Blots were probed with antibodies specific for B56α and the catalytic subunits of PP2A and PP1 as described under "Experimental Procedures." In addition, the B56α signal was identified by immunoprecipitation (*IP*), preincubating the affinity-purified rabbit B56α antibody (*ab*) with or without a blocking peptide (*pep.*) encoding the human full-length B56α (*lower panel*). Shown is the quantitation of PP subunits by densitometric scanning of immunoblots (*right panel*). *B*, total PP activity was measured in extracts of either ventricular (*Ventr.*) homogenates (*left panel*) or isolated cardiomyocytes (*right panel*) using ^{32}P-labeled phosphorylase *a* as substrate. Samples were also assayed in the presence of 3 nM okadaic acid, allowing the discrimination between PP2A and PP1 activities. *C*, PP activity was also determined in cardiac extracts incubated with increased concentrations of okadaic acid. Shown is the PP activity expressed as a percentage of control (*Ctr.*), which is the phosphatase activity in the absence of okadaic acid. *, $p < 0.05$ *versus* WT.

inhibiting only PP2A activity (13). PP2A activity was increased by almost 2-fold in TG compared with WT, which is in contrast to the unchanged PP1 activity between both groups (Fig. 1*B*). These data are consistent with the higher expression of the $PP2A_C$ protein in TG extracts. Measurement of PP activities in extracts of isolated cardiomyocytes revealed very comparable proportions between TG and WT, as well as similar specific PP activities as observed in ventricular preparations (Fig. 1*B*). Thus, it can be derived from these experiments that ventricular homogenates are highly representative for the conditions in ventricular cardiomyocytes and therefore were used for all further biochemical assays. The potency of okadaic acid to inhibit PP2A activity was decreased in TG because phosphatase activity was less strongly reduced at lower concentrations (<3 nM) of the toxin (Fig. 1*C*). This suggests that the predominance of

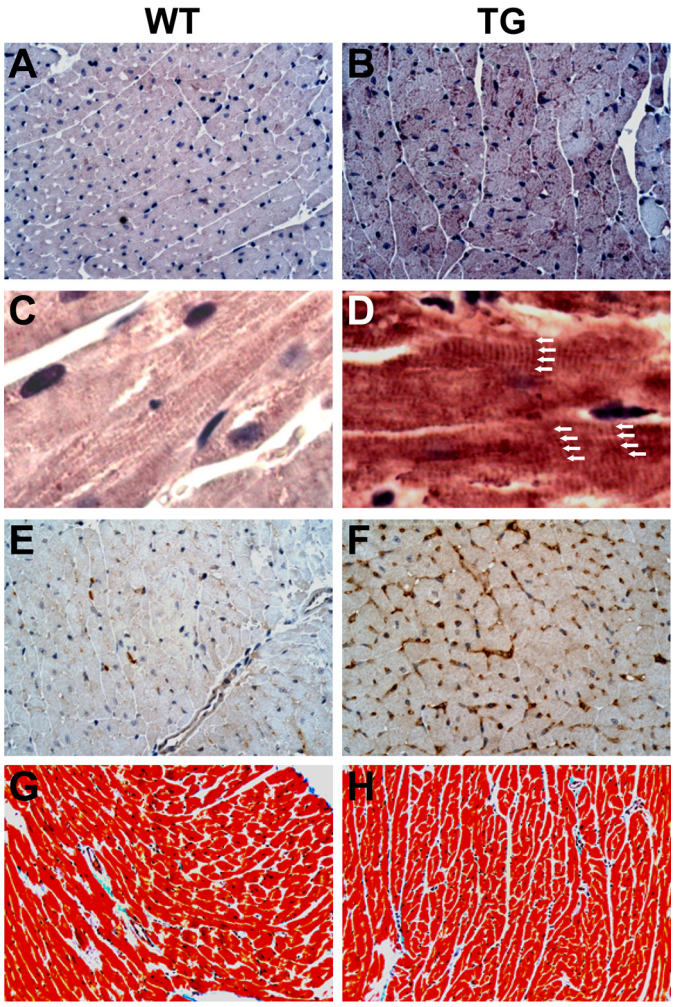

FIGURE 2. **Immunohistochemical detection of B56α and PP2A$_C$.** Sections from paraffin-embedded ventricular tissue of WT and TG mice were immunoreacted either with a rabbit polyclonal antibody that recognizes both endogenous mouse and exogenous human B56α (*A–D*) or with a rabbit polyclonal antibody raised against human PP2A$_C$ (*E* and *F*). *Arrows* indicate the sarcomeric localization of overexpressed B56α. Sections were also stained with Masson's trichrome to detect connective tissue (*G* and *H*).

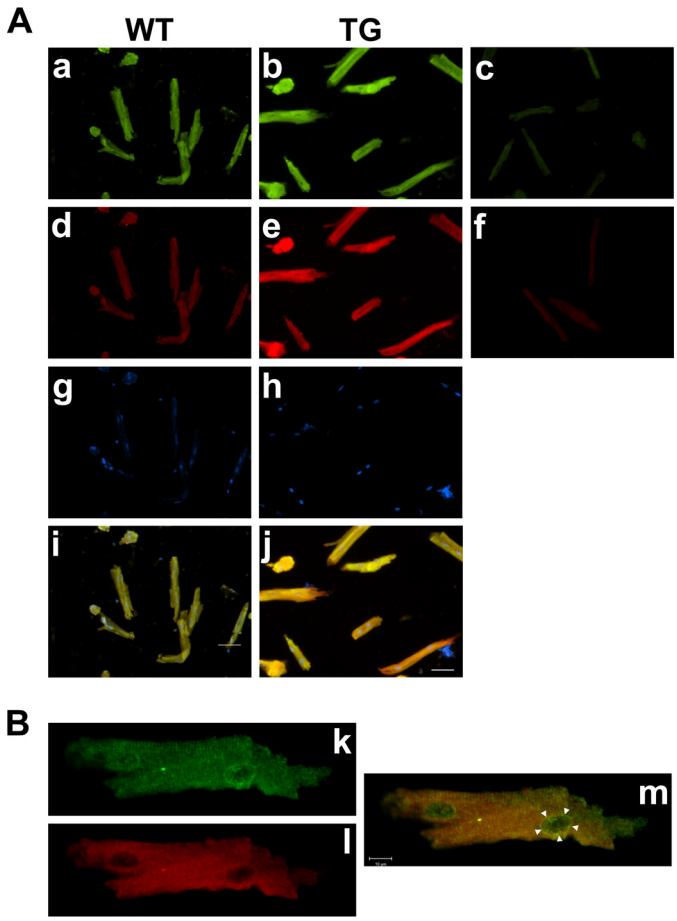

FIGURE 3. **Detection of B56α and PP2A$_C$ in cardiomyocytes by immunofluorescence.** *A*, photomicrographs showing isolated cardiomyocytes from WT (*panels a*, *c*, *d*, *f*, *g*, and *i*) and TG (*panels b*, *e*, *h*, and *j*) mouse hearts. *B*, photomicrographs showing detailed analysis of TG cardiomyocytes by confocal microscopy (*panels k–m*). In detail, green fluorescence staining of B56α (*panels a*, *b*, and *k*), red fluorescence staining of PP2A$_C$ (*panels d*, *e*, and *l*), control without primary antibodies (*panels c* and *f*), DAPI nuclei staining (*panels g* and *h*), and the overlay (*panels i*, *j*, and *m*). Note the increased signal of B56α and PP2A$_C$ in TG (*panels b* and *e*, respectively) compared with WT cardiomyocytes (*panels a* and *d*). Confocal analysis revealed a sarcomeric pattern in the distribution of B56α (*panel k*) and an enrichment of B56α in nuclear membranes (*white arrowheads*). *Scale bar*, 50 μm (*A*) and 10 μm (*B*).

PP2A activity may lead to functional effects on cardiac performance in TG mice.

PP2A Activity Is Enhanced in the Cytosol and Myofilaments of TG Cardiomyocytes—The subcellular distribution of B56α was assessed by immunostaining of sections from paraffin-embedded mouse hearts. Staining with an antibody that reacts with both endogenous mouse and transgenic human B56α showed the localization in the cytosol and myofilaments of TG and WT cardiomyocytes (Fig. 2, *A* and *B*). Magnification of stainings revealed a sarcomeric enhancement of the B56α signal in TG (Fig. 2, *C* and *D*). Immunostaining of heart sections using an antibody that recognizes the catalytic subunit of PP2A revealed a homogeneous distribution throughout the cardiomyocytes (Fig. 2, *E* and *F*), suggesting the co-localization of B56α and Cα in the cytosol. Cα was also detected in the nuclei of TG heart sections. The histological analysis revealed also no signs of fibrosis in TG compared with WT hearts (Fig. 2, *G* and *H*). Immunofluorescence staining of isolated cardiomyocytes showed increased protein levels of B56α and PP2A$_C$ in TG (Fig. 3*A*). Moreover, a detailed analysis of B56α and PP2A$_C$ distribution in cells by confocal laser scanning microscopy revealed a cytosolic and sarcomeric pattern of B56α in TG (Fig. 3*B*), whereas the fluorescence signal of the PP2A$_C$ exhibited a more equal distribution throughout the cells. Overall B56α and PP2A$_C$ co-localized in both the cytosol and the sarcomeric structure of TG cardiomyocytes (Fig. 3*B*). In the nuclei of TG cardiomyocytes, an increased amount of B56α was detected in the membrane. The subcellular localization of PP2A subunits was also assessed with immunoblot analysis (Fig. 4*A*). For this purpose we analyzed equivalent amounts of the cytosol, membrane, and myofilament fractions. The enrichment and purity of subcellular fractions (cytosol, myofilaments, and membranes) were tested by detection of specific marker proteins (myoglobin, TnI, and SERCA2a, respectively) (Fig. 4*A*). We found that B56α and the catalytic subunit of PP2A were present in the cytosol and the myofilaments, suggesting the co-localization of the transgene and Cα in mouse cardiomyocytes (Fig. 4, *A* and *B*). Moreover, B56α and the scaffolding subunit were

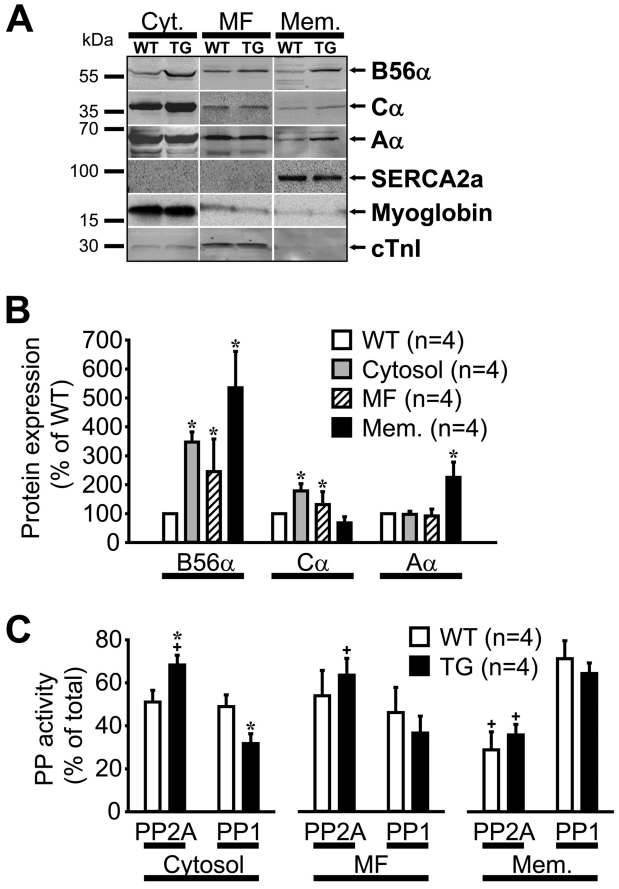

FIGURE 4. **Expression and activity of PP2A in myocardial fractions.** The expression of PP2A subunits was assessed in different myocellular compartments of WT and TG hearts (*A*). *Cyt.*, cytosol; *MF*, myofilaments; *Mem.*, membranes. The preparation of crude myocardial fractions was achieved by use of a differential centrifugation protocol. After SDS-PAGE, the separated proteins were transferred to nitrocellulose membranes. Thereafter, immunoblotting was performed to detect the regulatory (B56α), the catalytic (Cα), or the scaffolding (Aα) subunit of PP2A, as well as specific marker proteins, indicating the purity of myocardial fractions. Shown is the quantification of the protein expression of PP2A subunits in fractions prepared of mouse ventricles (*B*). PP activity was measured in cytosolic, myofilament, and membrane fractions in the absence and presence of 3 nM okadaic acid to differentiate between PP2A and PP1 activity (*C*). *, $p < 0.05$ *versus* WT; +, $p < 0.05$ *versus* PP1.

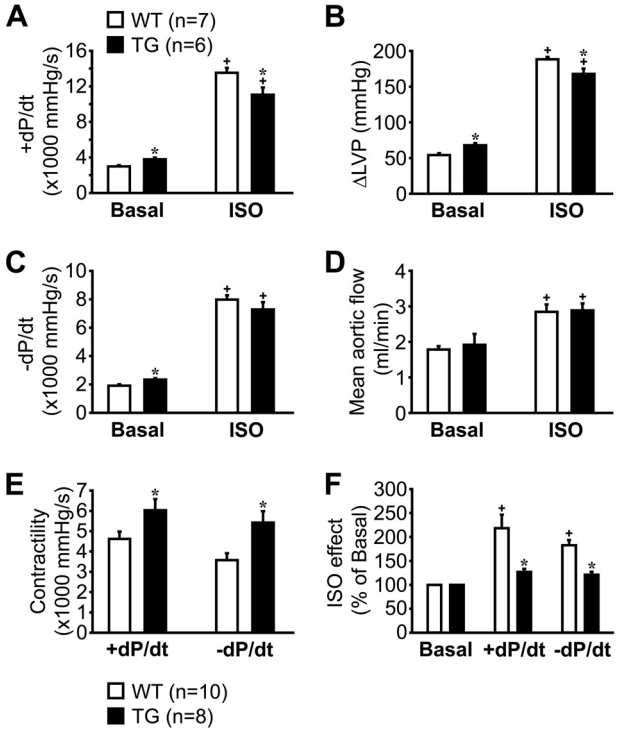

FIGURE 5. **Recording of contractile function on isolated hearts.** Isolated hearts of WT and B56α-overexpressing (TG) mice were perfused in the Langendorff mode. *A–D*, contractile parameters were recorded under basal conditions and after β-adrenergic stimulation. *A*, maximum rate of LV pressure development; *B*, maximum amplitude of LV pressure; *C*, maximum rate of LV pressure decline; *D*, mean aortic flow. *E* and *F*, basal (*E*) and ISO-stimulated (*F*) contractility was also studied on isolated mouse hearts at an afterload of 50 mm Hg using the work-performing mode. *, $p < 0.05$ *versus* WT; +, $p < 0.05$ *versus* basal.

enriched in membrane fractions of transgenic hearts (Fig. 4, *A* and *B*). These data indicate a targeting of PP2A activity by B56α overexpression to substrates localized mainly in the cytosol and myofilaments. We also tested whether the expression degree of PP2A subunits in subcellular fractions correlates with appropriate changes in phosphatase activity. Normally, the relation between PP2A to PP1 activity is balanced in WT cardiomyocytes. B56α overexpression resulted in an increased PP2A activity in the cytosol of TG compared with WT hearts, which is consistent with a higher ratio of PP2A to PP1 activity (Fig. 4*C*). This ratio was also enhanced in the myofilament fraction of TG compared with WT hearts (Fig. 4*C*). In contrast, the ratio of PP2A to PP1 activity was comparable between TG and WT membrane fractions (Fig. 4*C*).

Increased Basal Contractility but Blunted Effects after β-Adrenergic Stimulation in TG Hearts—The effects of B56α overexpression on cardiac performance was determined on isolated, beating Langendorff-perfused mouse hearts. To exclude changes in intrinsic heart rate that may affect contractility, hearts were stimulated with 8 Hz. The maximal rates of pressure development (+dP/dt) and the LV pressure amplitude (ΔLVP) were enhanced by 27 and 26%, respectively, under basal conditions in TG compared with WT hearts (Fig. 5, *A* and *B*). ISO administration resulted in higher contractile parameters (+dP/dt and ΔLVP) in both groups. However, this increase was less pronounced in TG (by 197 and 151%, respectively) compared with WT hearts (by 361 and 253%, respectively, $p < 0.05$; Fig. 5, *A* and *B*). The basal rate of relaxation (−dP/dt) was also increased by 22% in TG compared with WT hearts (Fig. 5*C*). The ISO-stimulated increase in the rate of relaxation was lower in TG (by 212%) compared with WT hearts (by 323%, $p < 0.05$; Fig. 5*C*). The mean aortic flow was unchanged between both groups under basal conditions and after β-adrenergic stimulation (Fig. 5*D*). Contractile parameters were also assessed at the whole heart level in the work performing mode. Under the basal loading conditions utilized (50 mm Hg aortic pressure), TG mice exhibited a higher contractility (Fig. 5*E*). The maximal rates of pressure development and relaxation were increased by 31 and 52%, respectively, in TG compared with WT hearts. The β-adrenergic response was markedly diminished in TG hearts. The rates of contraction and of relaxation were decreased by 42 and 34%, respectively, in TG compared with WT hearts (Fig. 5*F*).

Enhanced Ca^{2+} Sensitivity in TG Cardiomyocytes—To see whether contractile changes in TG hearts persisted to the cellular level, we measured Ca^{2+} transients and sarcomere length

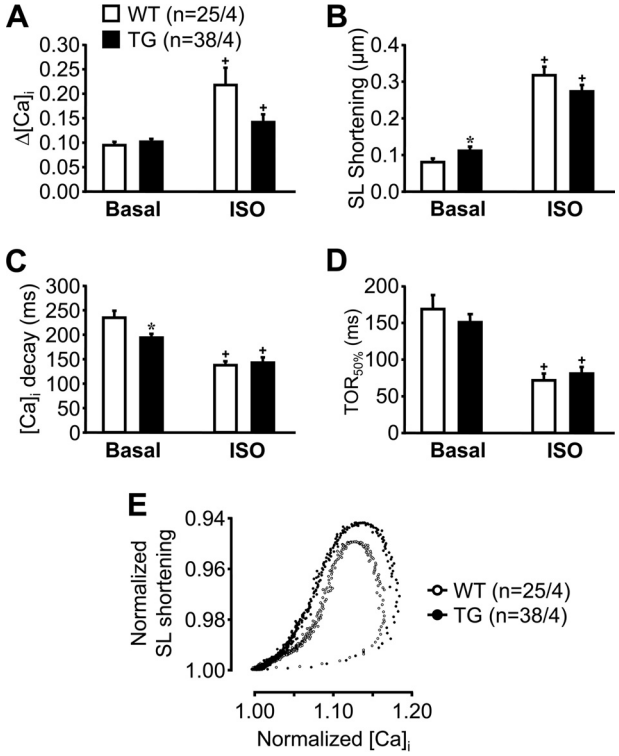

FIGURE 6. **Measurement of Ca^{2+} transients and sarcomere length in isolated cardiomyocytes.** Intracellular Ca^{2+} transients and cardiomyocyte contraction were measured simultaneously at 0.5-Hz stimulation frequency in isolated cardiomyocytes of WT and TG mice under basal conditions and after application of ISO. *A–D*, shown are the summarized data of $[Ca]_i$ peak amplitude (*A*), sarcomere length shortening (*B*), the time to 50% $[Ca]_i$ decay (*C*), and the time of 50% relaxation (*D*). *E*, the normalized data of basal $[Ca]_i$ peak amplitude and SL shortening were correlated. The slope of this relation can be used as an indicator of myofilament Ca^{2+} sensitivity. *, $p < 0.05$ *versus* WT; +, $p < 0.05$ *versus* basal.

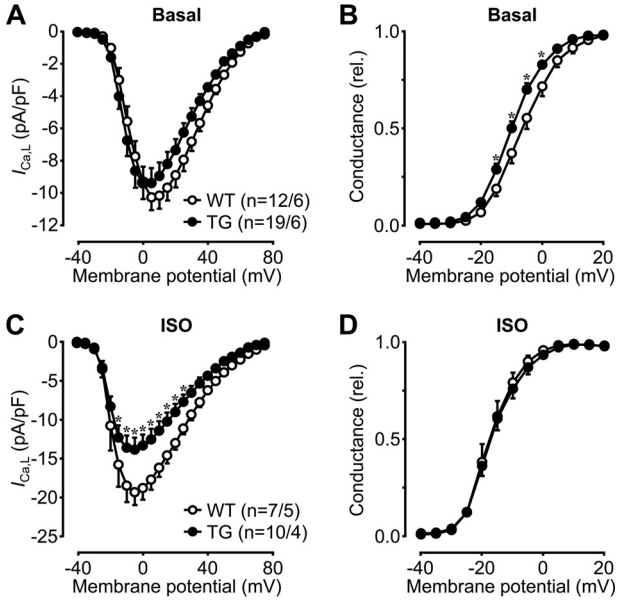

FIGURE 7. **Analysis of L-type Ca^{2+} channel currents in isolated cardiomyocytes.** The peak current-voltage relation was obtained from WT and TG cardiomyocytes under basal conditions (*A*) and after administration of ISO (*C*). L-type Ca^{2+} channels were activated by 400-ms depolarizing pulses after a prepulse to −40 mV to the indicated test potentials (−80 mV holding potential). Currents were related to individual cell capacitances. Shown is the conductance-voltage relation in the absence (*B*) and presence (*D*) of 1 μM ISO. The values were normalized to the maxima and fitted to a Boltzmann function. *, $p < 0.05$ *versus* WT, RM-analysis of variance with Holm-Sidak post hoc test.

(SL) shortening in perfused, isolated cardiomyocytes. The peak amplitude of $[Ca]_i$ was unchanged under basal conditions between TG and WT cardiomyocytes (Fig. 6*A*). The administration of maximum concentrations of ISO (1 μM) was associated with a lower increase of $\Delta[Ca]_i$ in TG (by 38%) compared with WT cardiomyocytes (by 129%, $p < 0.05$; Fig. 6*A*). The SL shortening was also simultaneously recorded in cardiomyocytes in the absence and presence of ISO (Fig. 6*B*). Interestingly, SL shortening was increased by 38% under basal conditions in TG compared with WT cardiomyocytes. The blunted increase in SL shortening after application of ISO in TG cardiomyocytes is consistent with changes in $\Delta[Ca]_i$. The increase in SL shortening after application of ISO was less pronounced in TG (by 145%) compared with WT cardiomyocytes (by 291%, $p < 0.05$; Fig. 6*B*). In addition, we have also recorded the decay kinetics in isolated cardiomyocytes. The time to 50% decay of $[Ca]_i$ was reduced by 18% in TG compared with WT cardiomyocytes under basal conditions. The application of ISO resulted in a lower reduction in $[Ca]_i$ decay kinetics in TG (by 24%) compared with WT (by 41%, $p < 0.05$; Fig. 6*C*). The time of relaxation was not different between WT and TG cardiomyocytes under basal conditions (Fig. 6*D*). The hastening of relaxation after administration of ISO was lower in TG (by 43%) compared with WT cardiomyocytes (by 57%; Fig. 6*D*) but did not reach statistical significance ($p = 0.088$). Overall, measurements in cardiomyocytes support the data obtained from isolated hearts, suggesting a blunted response to β-adrenergic stimulation in TG. The steeper course of the normalized $[Ca]_i$-sarcomere length relation suggests an increased myofilament Ca^{2+} sensitivity of TG compared with WT cardiomyocytes (Fig. 6*E*).

Reduced L-type Ca^{2+} Current Densities after ISO Stimulation in TG Cardiomyocytes—To test whether the altered Ca^{2+} transients under basal conditions and after β-adrenergic stimulation in TG cardiomyocytes were accompanied by changes in the trigger for the SR Ca^{2+} release, we measured the L-type Ca^{2+} current ($I_{Ca,L}$) in isolated cardiomyocytes. Cell membrane capacitance was comparable in TG and WT cardiomyocytes (data not shown). This is consistent with a normal cell morphology observed in the histological examination. At basal conditions, the normalized $I_{Ca,L}$ current densities were not different between TG and WT cardiomyocytes, but the TG I-V-curve was slightly left-shifted (Fig. 7*A*). This was associated with a left shift in the corresponding TG steady-state activation curve compared with the WT curve (Fig. 7*B*) ($V_{½}$: WT = −6.0 mV, TG = −9.4 mV). L-type Ca^{2+} currents were also measured after application of ISO (Fig. 7*C*). At depolarizing potentials between −15 and +25 mV, the normalized $I_{Ca,L}$ current densities were reduced in TG compared with WT cardiomyocytes. ISO shifted the voltage dependence of $I_{Ca,L}$ activation to more negative E_m (Fig. 7*D*). However, the ISO activation curves were not different between both groups ($V_{½}$: WT = −15.9 mV, TG = −16.0 mV).

Lower Phosphorylation of Myofilament Proteins in TG Hearts—To investigate whether the altered Ca^{2+} handling and the increased myofilament Ca^{2+} sensitivity in TG cardiomyocytes are associated with corresponding changes of mRNA and

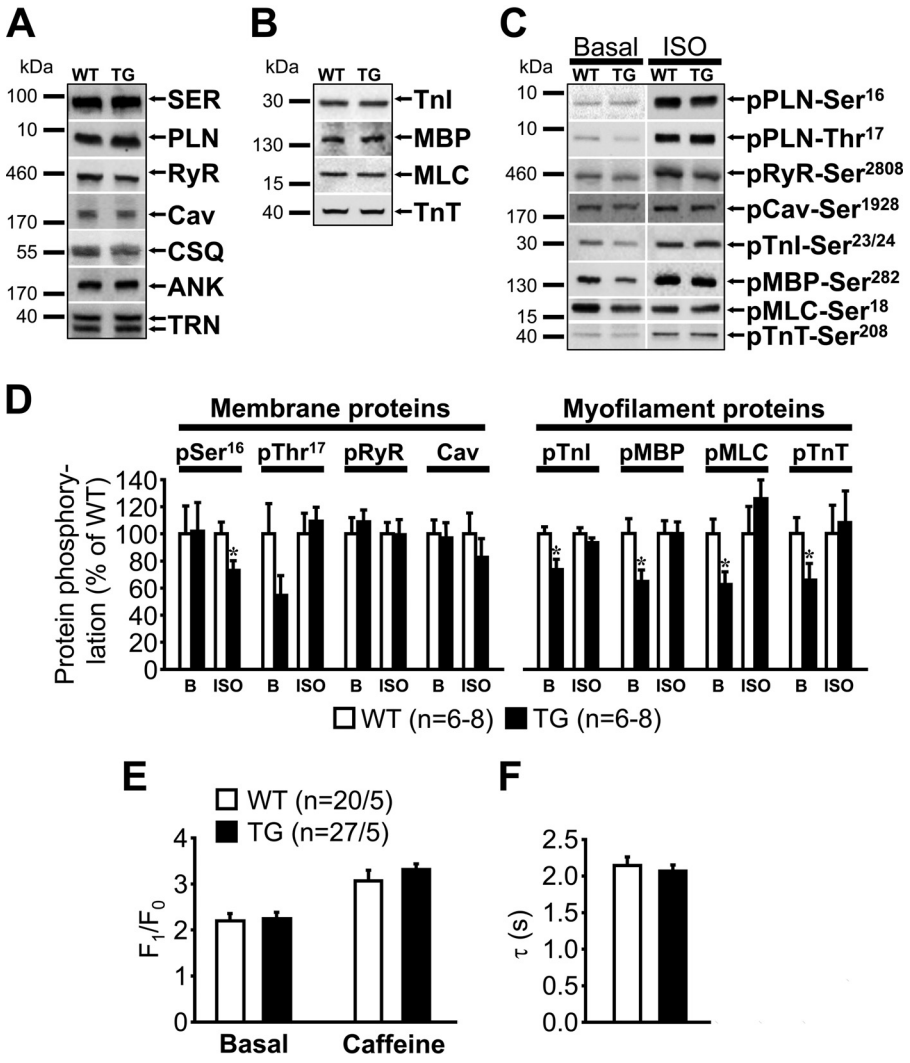

FIGURE 8. **Expression of regulatory proteins in crude heart homogenates.** Mouse heart tissue from WT and B56α-overexpressing (TG) mice was homogenized, and solubilized proteins were separated on polyacrylamide gels. After the transfer to nitrocellulose membranes, blots were consecutively probed with specific antibodies directed against either membrane-associated proteins (*A*) or myofilament regulatory proteins (*B*). Homogenates were also prepared from Langendorff-perfused hearts treated with ISO to obtain a maximum β-adrenergic stimulation. Samples were analyzed by SDS-PAGE, and blots were consecutively probed with phospho-specific antibodies as described under "Experimental Procedures." Shown are representative immunoblots (*C*) and the quantitative analysis of phosphorylated regulatory membrane-associated (sarcolemma or SR) and myofilament proteins under basal (*bars* labeled *B*) and ISO-stimulated conditions (*D*). Caffeine-induced Ca^{2+} release was determined in isolated cardiomyocytes that were loaded with Fluo-4. Shown are F_1/F_0 peak amplitudes and decay kinetics (*E*). *Cav*, L-type Ca^{2+} channel; *SER*, sarco(endo)plasmic reticulum Ca^{2+} ATPase; *RyR*, ryanodine receptor; *CSQ*, calsequestrin; *ANK*, ankyrin B; *TRN*, triadin 1. *, $p < 0.05$ *versus* WT.

protein expression levels of Ca^{2+} regulatory proteins, we performed quantitative RT-PCR analysis and immunoblotted cardiac homogenates from both groups, using an array of antibodies raised to SR and myofilament proteins, respectively (Fig. 8, *A* and *B*). Overall mRNA levels of all membrane-associated genes exhibited no differences between both groups (Table 1). Expression levels of sarcolemmal Cav1.2 or SR proteins (SERCA2a, phospholamban (PLN), calsequestrin, ryanodine receptor, and triadin 1) were unaltered in TG hearts (Table 2). An unchanged protein expression was also observed for ankyrin B, which is thought to be responsible for the tethering of PP2A to some of their substrates (Table 2). Moreover, we analyzed proteins arising from cardiac myofilaments. The expression levels of the troponin inhibitor (TnI), myosin-binding protein C (MyBP-C), myosin light chain 2 (MLC-2), and TnT were similar between TG and WT hearts (Table 2). In addition, we tested the phosphorylation state of different Ca^{2+} regulatory proteins (Fig. 8*C*). We found an unchanged phosphorylation level of Cav1.2 at basal and ISO-stimulated conditions between TG and WT (Fig. 8*D*). The phosphorylation state of PLN at Ser^{16} and of the ryanodine receptor at Ser^{2808} was comparable under basal conditions in both groups (Fig. 8*D*). The application of ISO was associated with a lower phosphorylation state of PLN at Ser^{16} in TG compared with WT. Interestingly, cardiomyocyte-directed overexpression of B56α resulted in a decreased phosphorylation state of all myofilament proteins assessed, namely TnI at $Ser^{23/24}$, MyBP-C at Ser^{282}, MLC-2 at Ser^{18}, and TnT at Ser^{208}, under basal conditions. In contrast, the phosphorylation state of these proteins was not different after administration of ISO in TG compared with WT hearts (Fig. 8*D*). Next, we examined the activity of PKA regulating the phosphorylation state of main cardiac Ca^{2+}

TABLE 1

Quantification of mRNA levels of membrane-associated proteins in cardiomyocytes

Relative expression ratios of TG *versus* WT cardiomyocytes were calculated by the relative expression software tool (REST, version 2.0.13), using *Hprt* mRNA as a reference gene and a statistical randomization test analysis ($n = 5–6$).

Gene	TG *vs.* WT	S.E.	Primer pairs	
			Forward	Reverse
Hprt	1		5′-atgagcgcaagttgaatctg-3′	5′-ggacgcagcaactgacatt-3′
Atp2a2	0.95	0.74–1.19	5′-ctgtggagacccttggttgt-3′	5′-cagagcacagatggtggcta-3′
Pln	0.95	0.80–1.23	5′-ttggaaacaggtttgcatga-3′	5′-tcacgtttctctcagcatgg-3′
Ryr2	0.95	0.66–1.93	5′-taatggtctccttgcagcca-3′	5′-ttcggatggcttctcccttt-3′
Cacna1c	0.88	0.56–1.48	5′-ctttgcggagaagagtgacc-3′	5′-acattcaccaccccaatctg-3′
Casq2	0.88	0.63–1.32	5′-ctttgcggagaagagtgacc-3′	5′-acattcaccaccccaatctg-3′
Ank2	0.94	0.63–1.29	5′-aggtggtcagattgatgcca-3′	5′-gccttgtattggagcaggtg-3′
Trdn	0.95	0.77–1.24	5′-aagagcccttgtcatacccc-3′	5′-gacagacctcttcagcacct-3′

TABLE 2

Quantification of protein expression

Levels of cardiac regulatory SR and myofilament proteins in homogenates of WT and TG mouse hearts were measured after scanning ECL-labeled immunoblots in a ChemiDoc XRS system (Bio-Rad).

Protein	WT	TG	*n*
	%	%	
Cav1.2	100.0 ± 7.2	101.1 ± 7.1	15
SERCA2a	100.0 ± 6.2	111.0 ± 3.5	7
Phospholamban	100.0 ± 11.3	106.5 ± 7.6	12
Ryanodine receptor	100.0 ± 8.1	87.6 ± 6.4	12
Calsequestrin	100.0 ± 5.4	101.9 ± 5.5	7
Ankyrin B	100.0 ± 4.2	100.6 ± 3.8	15
Triadin	100.0 ± 3.6	101.7 ± 6.9	7
Troponin inhibitor	100.0 ± 4.1	102.4 ± 2.4	15
Troponin T	100.0 ± 4.8	97.4 ± 5.0	7
Myosin light chain 2	100.0 ± 4.9	103.3 ± 3.7	15
Myosin-binding protein C	100.0 ± 7.3	96.5 ± 6.1	15

regulatory proteins. The basal enzymatic activity of PKA was enhanced by 28% in TG compared with WT myocardium (290.5 ± 16.4 *versus* 226.5 ± 13.1 pmol/mg/min, $p < 0.05$, $n = 7–8$). Maximal stimulation of PKA activity with cAMP was comparable in both groups (ratio of −cAMP/+cAMP: 0.122 ± 0.006 *versus* 0.129 ± 0.004, not significant, $n = 7–8$). To assess the SR Ca^{2+} content, caffeine-induced Ca^{2+} transients were measured in isolated cardiomyocytes. The basal twitch $[Ca]_i$ peak amplitude was unchanged between TG and WT (Fig. 8*E*). The caffeine-triggered peak amplitude of $[Ca]_i$ was also not different between both groups, indicating a similar SR Ca^{2+} load in TG and WT (Fig. 8*E*). These data are consistent with the unchanged expression level of SR proteins at basal conditions. Furthermore, the time constant of decline of caffeine-dependent $[Ca]_i$ was comparable in TG and WT (Fig. 8*F*), suggesting a normal function of the Na/Ca exchanger.

DISCUSSION

B56α is the main regulatory subunit of PP2A in cardiac cardiomyocytes (10, 11), where it appears to regulate the interaction between the PP2A heterodimer and its targeting substrates, thereby mediating the dephosphorylation of important regulatory proteins like the L-type Ca^{2+} channel, cTnI, or PLN. Thus, we hypothesized that an increased expression of B56α in the heart may influence cardiac performance by altering subcellular localization of PP2A. Here we generated a transgenic mouse model to show that cardiac-specific overexpression of B56α was associated with redistribution of $PP2A_C$ expression/activity in the cytosol and myofilaments, dephosphorylation of sarcomeric proteins, increased Ca^{2+} sensitivity, and higher contractility. In contrast, overexpression of B56α led to an impaired contractile response to β-adrenergic stimulation.

In the present study, overexpression of B56α in the heart led to a concomitant increase in the expression of the PP2A catalytic subunit. This effect seems to be limited to the long term expression of B56α, whereas the short term expression of this regulatory subunit in either adenovirus-infected rat cardiomyocytes (15) or transfected HEK293 cells (13) did not alter $PP2A_C$ levels. Interestingly, cardiomyocyte-directed overexpression of the catalytic subunit was not followed by an increase in the protein expression of B56α and $PP2A_A$, as well (7). We have recently demonstrated that wild-type B56α is a potent inhibitor of PP2A activity (13). The phosphatase 2A was completely inhibited by B56α at concentrations of ~100 nM. This suggests a compensatory up-regulation of $PP2A_C$ expression in B56α-overexpressing hearts. On the other hand, it could be that the desensitization of PP2A in transgenic hearts occurs as a mechanism to offset the 2-fold increase in PP2A activity. Thus, the time-dependent adaptation of $PP2A_C$ expression in B56α-overexpressing mice may help to maintain the dynamic equilibrium between myocellular protein kinases and PP2A as close to normal as possible.

Because most of the models with an enhanced expression of $PP2A_C$ are associated with cardiac hypertrophy and contractile failure (7, 31–34), we designed several experiments to determine heart performance in isolated organs and cardiomyocytes of mice with B56α overexpression. Surprisingly, cardiac contractility was higher in all experimental settings studied, namely in isolated, electrically stimulated Langendorff-perfused hearts, work-performing heart preparations, and cardiomyocytes of transgenic mice. What might explain these differences in cardiac performance despite a comparable increase in $PP2A_C$ expression and/or activity? In previous studies, the impairment of heart function was paralleled by a reduced phosphorylation of cTnI, PLN, and connexin43, suggesting a PP2A-dependent dephosphorylation of several phosphoproteins that are located in organelles throughout the cardiomyocyte. Overall, this resulted in a disturbed myocellular Ca^{2+} handling. In the present study, we also found a dephosphorylation of PP2A substrates. However, the reduced phosphorylation was strictly confined to myofilament proteins (*e.g.* cTnI, MyBP-C) in B56α-overexpressing mice, whereas membrane-associated sarcolemmal (Cav1.2) and SR (*e.g.* RyR) proteins exhibited an unchanged phosphorylation status, suggesting that this regulatory PP2A subunit is not functionally active in targeting PP2Ac activity to

membrane-associated proteins like ion channels despite increased levels of B56α in the membrane-enriched fraction of TG hearts. It can be suggested from immunofluorescence studies that the detection of B56α in the membrane fraction may originate from its increased expression in nuclear membranes of TG cardiomyocytes. The dephosphorylation of myofibrillar proteins was associated with a redistribution of the $PP2A_C$-B56α complex to the cytosol and myofilament fractions, resulting in an overall higher PP2A/PP1 ratio in transgenic compared with wild-type sarcomeres, as indicated by our (immuno)cellular and biochemical studies. In myofilaments, PP2A has been localized to the Z-disc, where it comes in proximity to the A- and I-band regions of the sarcomere (16, 35). This suggests that overexpression of B56α forwards the targeting of the PP2A holoenzyme to specific myofilament proteins. Consistently, adenovirus-mediated expression of B56α in cultured neonatal ventricular cardiomyocytes displayed a striated intracellular pattern (15). On the other hand, microRNA-dependent reduction of B56α resulted in a higher phosphorylation of the ryanodine receptor and the L-type Ca^{2+} channel via disrupting localization of PP2A activity to these channels (36, 37). This effect was associated with abnormal intracellular Ca^{2+} cycling and an increased propensity to arrhythmogenesis. Because targeting of $PP2A_C$-B56α activities to specialized subcellular domains also depends on specific adapter proteins, we measured the protein expression of ankyrin B. The reduced expression of ankyrin B in primary cardiomyocytes resulted in disorganized distribution of B56α (14). However, ankyrin B expression was not different between B56α-overexpressing and wild-type hearts, excluding an influence on PP2A targeting in our transgenic model.

Our major finding is that B56α overexpression enhanced cardiac performance, although the peak amplitude of intracellular Ca^{2+} transients was comparable between transgenic and wild-type cardiomyocytes. The increased myofilament Ca^{2+} sensitivity is attributable to a diminished phosphorylation of myofilament regulatory proteins. The hypophosphorylation of cardiac TnI, MyBP-C, MLC-2, and TnT is likely to be due to the higher PP2A activity in myofilament fractions. PP2A induced uniform dephosphorylation of cTnI in preparations previously treated with both PKA and PKC (38). We have recently demonstrated that the administration of purified $PP2A_C$ dephosphorylated cTnI at PKA sites $Ser^{23/24}$, resulting in an increased Ca^{2+} sensitivity of the contractile apparatus in isolated skinned human cardiomyocytes (39). A decreased cTnI phosphorylation at PKA-dependent phosphosites was also found in a dog heart failure model (40). The hypophosphorylation was associated with a higher PP2A expression/activity, as observed in our transgenic mouse model. This might explain the increased myofilament Ca^{2+} sensitivity in skinned cardiomyocytes. Hence, there seems to be a causal link between higher expression of $PP2A_C$-B56α, hypophosphorylation of myofilament proteins, and increased Ca^{2+} sensitivity and contractile force. This is also supported by the fact that, on the other hand, an increased cTnI phosphorylation at $Ser^{23/24}$ and a decrease in myofilament Ca^{2+} sensitivity in LPS-induced septic hearts was paralleled by a reduction in the expression of $PP2A_C$-B56α, resulting in an overall decreased PP2A activity (17). Taken together, these studies support the hypothesis that B56α is a crucial modulator of cardiac Ca^{2+} sensitivity and contractility by influencing the PP2A-dependent dephosphorylation of regulatory myofilament proteins. This targeting function of B56α might also explain the absence of cardiomyocyte hypertrophy in TG hearts, which is in contrast to other heart failure models that exhibit a nontargeted myocellular elevation of PP2A activity (7). In addition, it has been shown that not only phosphorylation of cTnI, but also phosphorylation of other contractile proteins regulates myofilament Ca^{2+} sensitivity. In the present study, we found also a diminished phosphorylation of cardiac MyBP-C, MLC-2, and TnT. PKA-dependent phosphorylation of cMyBP-C results in the reduction in myofilament Ca^{2+} sensitivity and the attenuation in myofilament force. This is due to an increased rate of cross-bridge detachment (41). Consistently, a higher Ca^{2+} sensitivity was measured in a mouse model lacking cMyBP-C (42). Because PP2A is the major phosphatase controlling dephosphorylation of cMyBP-C (43), we suggest that the reduced phosphorylation of this thick filament protein may also contribute, at least in part, to the enhanced Ca^{2+} sensitivity and cardiomyocyte contractility in B56α-overexpressing mice. Moreover, it can be suggested that the hypophosphorylation of cardiac MLC-2 and TnT may also influence the functional effects observed in transgenic mice with B56α overexpression. The significance of PP2A-dependent dephosphorylation of cTnT has been implicated by Wu and Solaro (44), who reported that cTnT exists in a complex with PKCζ, Pak1, and PP2A. Recently, Ser^{208} of cTnT was identified as the potential phosphosite that can be dephosphorylated by PP2A (29). Moreover, the increased Ca^{2+} sensitivity of force in remote tissue from grafted hearts was explained by a reduced phosphorylation of cardiac TnT and/or MLC-2 (45). Thus, the $PP2A_C$-B56α-dependent hypophosphorylation of these regulatory myofilament proteins may contribute to the higher Ca^{2+} sensitivity observed in TG cardiomyocytes.

PP2A reverses the action of protein kinases after activation of the β-adrenergic signaling pathway in cardiac cardiomyocytes. Moreover, PP2A activity itself is regulated by a PKA-dependent phosphorylation of its regulatory B subunits after sympathetic activation, serving as a feedback mechanism on phosphorylated targets (13, 46, 47). Therefore, we studied cardiac function in B56α-overexpressing mice in response to β-adrenergic stimulation. Interestingly, we found a blunted contractile response to ISO in transgenic mice. This effect was observed in isolated heart preparations, as well as in single cardiomyocytes. The impaired response to β-adrenergic receptor stimulation was associated with similar changes in the intracellular Ca^{2+} handling. In detail, the increase in the peak amplitude of $[Ca]_i$ and the hastening of Ca^{2+} transient kinetics were reduced after application of ISO in TG. This can be attributed to the lower phosphorylation of PLN at Ser^{16} in B56α-overexpressing hearts after β-adrenergic stimulation, which is a common feature of failing heart models and also of failing human hearts (48). The reduced phosphorylation of PLN correlates with a decrease in the Ca^{2+} sensitivity of SERCA2a (49), resulting in an impaired SR Ca^{2+} uptake that contributes to the contractile failure. Here, the SR Ca^{2+} load was not altered in transgenic mice. Because a defective Ca^{2+} handling in failing cardiomyocytes is due to

sympathetic overactivity that affects β-adrenergic signaling upstream of PLN, we measured the activation state of PKA in the presence of cAMP. However, there is no evidence for a maladaptive response of the β-adrenergic pathway to an altered activity of protein kinases. Therefore, the hypophosphorylation of PLN after administration of ISO is rather due to an enhanced dephosphorylation by PP2A. Indeed, β-adrenergic stimulation resulted in a shift of $PP2A_C$-B56α activity from the myofilament fraction into the cytosol (16). This might explain the unchanged phosphorylation status of all myofilament proteins after ISO application between transgenic and wild-type heart homogenates. These dynamic changes of B56α-dependent targeting of PP2A may also account for the decreased current density of $I_{Ca,L}$ after β-adrenergic stimulation in cardiomyocytes with B56α overexpression. By use of phosphatase inhibitors, it has been shown that PP2A regulates the activity of L-type Ca^{2+} channels (4, 50). PP2A seems to dephosphorylate the channel at Ser^{1928}, the main PKA phosphosite (51).

In summary, this is the first study providing evidence that B56α directly regulates Ca^{2+} sensitivity, and thereby cardiac contractility, most likely by targeting PP2A to myocellular domains. This enables a coordinated stimuli-dependent dephosphorylation of specific substrates that regulate contractile response.

Acknowledgments—We thank N. Hinsenhofen and N. Nordsiek-Goda for excellent technical assistance.

REFERENCES

1. Liu, Q., and Hofmann, P. A. (2002) Antiadrenergic effects of adenosine A_1 receptor-mediated protein phosphatase 2a activation in the heart. *Am. J. Physiol. Heart Circ. Physiol.* **283,** H1314–H1321
2. Marx, S. O., Reiken, S., Hisamatsu, Y., Jayaraman, T., Burkhoff, D., Rosemblit, N., and Marks, A. R. (2000) PKA phosphorylation dissociates FKBP12.6 from the calcium release channel (ryanodine receptor): defective regulation in failing hearts. *Cell* **101,** 365–376
3. Davare, M. A., Horne, M. C., and Hell, J. W. (2000) Protein phosphatase 2A is associated with class C L-type calcium channels (Cav1.2) and antagonizes channel phosphorylation by cAMP-dependent protein kinase. *J. Biol. Chem.* **275,** 39710–39717
4. duBell, W. H., Lederer, W. J., and Rogers, T. B. (1996) Dynamic modulation of excitation-contraction coupling by protein phosphatases in rat ventricular myocytes. *J. Physiol.* **493,** 793–800
5. Neumann, J., Maas, R., Bokník, P., Jones, L. R., Zimmermann, N., and Scholz, H. (1999) Pharmacological characterization of protein phosphatase activities in preparations from failing human hearts. *J. Pharmacol. Exp. Ther.* **289,** 188–193
6. Bokník, P., Khorchidi, S., Bodor, G. S., Huke, S., Knapp, J., Linck, B., Lüss, H., Müller, F. U., Schmitz, W., and Neumann, J. (2001) Role of protein phosphatases in regulation of cardiac inotropy and relaxation. *Am. J. Physiol. Heart Circ. Physiol.* **280,** H786–H794
7. Gergs, U., Boknik, P., Buchwalow, I., Fabritz, L., Matus, M., Justus, I., Hanske, G., Schmitz, W., and Neumann, J. (2004) Overexpression of the catalytic subunit of protein phosphatase 2A impairs cardiac function. *J. Biol. Chem.* **279,** 40827–40834
8. Janssens, V., and Goris, J. (2001) Protein phosphatase 2A. A highly regulated family of serine/threonine phosphatases implicated in cell growth and signalling. *Biochem. J.* **353,** 417–439
9. Heijman, J., Dewenter, M., El-Armouche, A., and Dobrev, D. (2013) Function and regulation of serine/threonine phosphatases in the healthy and diseased heart. *J. Mol. Cell Cardiol.* **64,** 90–98
10. McCright, B., and Virshup, D. M. (1995) Identification of a new family of protein phosphatase 2A regulatory subunits. *J. Biol. Chem.* **270,** 26123–26128
11. DeGrande, S. T., Little, S. C., Nixon, D. J., Wright, P., Snyder, J., Dun, W., Murphy, N., Kilic, A., Higgins, R., Binkley, P. F., Boyden, P. A., Carnes, C. A., Anderson, M. E., Hund, T. J., and Mohler, P. J. (2013) Molecular mechanisms underlying cardiac protein phosphatase 2A regulation in heart. *J. Biol. Chem.* **288,** 1032–1046
12. McCright, B., Rivers, A. M., Audlin, S., and Virshup, D. M. (1996) The B56 family of protein phosphatase 2A (PP2A) regulatory subunits encodes differentiation-induced phosphoproteins that target PP2A to both nucleus and cytoplasm. *J. Biol. Chem.* **271,** 22081–22089
13. Kirchhefer, U., Heinick, A., König, S., Kristensen, T., Müller, F. U., Seidl, M. D., and Boknik, P. (2014) Protein phosphatase 2A is regulated by protein kinase Cα (PKCα)-dependent phosphorylation of its targeting subunit B56α at Ser^{41}. *J. Biol. Chem.* **289,** 163–176
14. Bhasin, N., Cunha, S. R., Mudannayake, M., Gigena, M. S., Rogers, T. B., and Mohler, P. J. (2007) Molecular basis for PP2A regulatory subunit B56α targeting in cardiomyocytes. *Am. J. Physiol. Heart Circ. Physiol.* **293,** H109–H119
15. Gigena, M. S., Ito, A., Nojima, H., and Rogers, T. B. (2005) A B56 regulatory subunit of protein phosphatase 2A localize to nuclear speckles in cardiomyocytes. *Am. J. Physiol. Heart Circ. Physiol.* **289,** H285–H294
16. Yin, X., Cuello, F., Mayr, U., Hao, Z., Hornshaw, M., Ehler, E., Avkiran, M., and Mayr, M. (2010) Proteomics analysis of the cardiac myofilament subproteome reveals dynamic alterations in phosphatase subunit distribution. *Mol. Cell Proteomics* **9,** 497–509
17. Marshall, M., Anilkumar, N., Layland, J., Walker, S. J., Kentish, J. C., Shah, A. M., and Cave, A. C. (2009) Protein phosphatase 2A contributes to the cardiac dysfunction induced by endotoxemia. *Cardiovasc. Res.* **82,** 67–76
18. Gulick, J., Subramaniam, A., Neumann, J., and Robbins, J. (1991) Isolation and characterization of the mouse cardiac myosin heavy chain genes. *J. Biol. Chem.* **266,** 9180–9185
19. Rapundalo, S. T., Solaro, R. J., and Kranias, E. G. (1989) Inotropic responses to isoproterenol and phosphodiesterase inhibitors in intact guinea pig hearts: comparison of cyclic AMP levels and phosphorylation of sarcoplasmic reticulum and myofibrillar proteins. *Circ. Res.* **64,** 104–111
20. Solaro, R. J., Pang, D. C., and Briggs, F. N. (1971) The purification of cardiac myofibrils with Triton X-100. *Biochim. Biophys. Acta* **245,** 259–262
21. Neumann, J., Boknik, P., Herzig, S., Schmitz, W., Scholz, H., Gupta, R. C., and Watanabe, A. M. (1993) Evidence for physiological functions of protein phosphatases in the heart: evaluation with okadaic acid. *Am. J. Physiol.* **265,** H257–H266
22. Kirchhefer, U., Neumann, J., Baba, H. A., Begrow, F., Kobayashi, Y. M., Reinke, U., Schmitz, W., and Jones, L. R. (2001) Cardiac hypertrophy and impaired relaxation in transgenic mice overexpressing triadin 1. *J. Biol. Chem.* **276,** 4142–4149
23. Kučerová, D., Baba, H. A., Bokník, P., Fabritz, L., Heinick, A., Mát'uš, M., Müller, F. U., Neumann, J., Schmitz, W., and Kirchhefer, U. (2012) Modulation of SR Ca^{2+} release by the triadin-to-calsequestrin ratio in ventricular myocytes. *Am. J. Physiol. Heart Circ. Physiol.* **302,** H2008–H2017
24. Schulte, J. S., Seidl, M. D., Nunes, F., Freese, C., Schneider, M., Schmitz, W., and Müller, F. U. (2012) CREB critically regulates action potential shape and duration in the adult mouse ventricle. *Am. J. Physiol. Heart Circ. Physiol.* **302,** H1998–H2007
25. Laemmli, U. K. (1970) Cleavage of structural proteins during the assembly of the head of bacteriophage T4. *Nature* **227,** 680–685
26. Porzio, M. A., and Pearson, A. M. (1977) Improved resolution of myofibrillar proteins with sodium dodecyl sulfate-polyacrylamide gel electrophoresis. *Biochim. Biophys. Acta* **490,** 27–34
27. Kobayashi, Y. M., and Jones, L. R. (1999) Identification of triadin 1 as the predominant triadin isoform expressed in mammalian myocardium. *J. Biol. Chem.* **274,** 28660–28668
28. Zhang, L., Kelley, J., Schmeisser, G., Kobayashi, Y. M., and Jones, L. R. (1997) Complex formation between junctin, triadin, calsequestrin, and the ryanodine receptor. *J. Biol. Chem.* **272,** 23389–23397
29. Dubois, E., Richard, V., Mulder, P., Lamblin, N., Drobecq, H., Henry, J.-P.,

Amouyel, P., Thuillez, C., Bauters, C., and Pinet, F. (2011) Decreased serine^{207} phosphorylation of troponin T as a biomarker for left ventricular remodeling after myocardial infarction. *Eur. Heart J.* **32,** 115–123

30. Kirchhefer, U., Schmitz, W., Scholz, H., and Neumann, J. (1999) Activity of cAMP-dependent protein kinase and Ca^{2+}/calmodulin-dependent protein kinase in failing and nonfailing human hearts. *Cardiovasc. Res.* **42,** 254–261
31. Bokník, P., Fockenbrock, M., Herzig, S., Knapp, J., Linck, B., Lüss, H., Müller, F. U., Müller, T., Schmitz, W., Schröder, F., and Neumann, J. (2000) Protein phosphatase activity is increased in a rat model of long-term β-adrenergic stimulation. *Naunyn-Schmiedebergs Arch. Pharmacol.* **362,** 222–231
32. Ai, X., and Pogwizd, S. M. (2005) Connexin 43 downregulation and dephosphorylation in nonischemic heart failure is associated with enhanced colocalized protein phosphatase type 2A. *Circ. Res.* **96,** 54–63
33. Larsen, K.-O., Lygren, B., Sjaastad, I., Krobert, K. A., Arnkvaern, K., Florholmen, G., Larsen, A.-K., Levy, F. O., Taskén, K., Skjønsberg, O. H., and Christensen, G. (2008) Diastolic dysfunction in alveolar hypoxia: a role for interleukin-18-mediated increase in protein phosphatase 2A. *Cardiovasc. Res.* **80,** 47–54
34. Golden, H. B., Watson, L. E., Nizamutdinov, D., Feng, H., Gerilechaogetu, F., Lal, H., Verma, S. K., Mukhopadhyay, S., Foster, D. M., Dillmann, W. H., and Dostal, D. E. (2013) Anthrax lethal toxin induces acute diastolic dysfunction in rats through disruption of the phospholamban signaling network. *Int. J. Cardiol.* **168,** 3884–3895
35. Yang, F., Aiello, D. L., and Pyle, W. G. (2008) Cardiac myofilament regulation by protein phosphatase type 1α and CapZ. *Biochem. Cell Biol.* **86,** 70–78
36. Terentyev, D., Belevych, A. E., Terentyeva, R., Martin, M. M., Malana, G. E., Kuhn, D. E., Abdellatif, M., Feldman, D. S., Elton, T. S., and Györke, S. (2009) Mir-1 overexpression enhances Ca^{2+} release and promotes cardiac arrhythmogenesis by targeting PP2A regulatory subunit B56α and causing CaMKII-dependent hyperphosphorylation of RyR2. *Circ. Res.* **104,** 514–521
37. Belevych, A. E., Sansom, S. E., Terentyeva, R., Ho, H. T., Nishijima, Y., Martin, M. M., Jindal, H. K., Rochira, J. A., Kunitomo, Y., Abdellatif, M., Carnes, C. A., Elton, T. S., Györke, S., and Terentyev, D. (2011) Microrna-1 and -133 increase arrhythmogenesis in heart failure by dissociating phosphatase activity from RyR2 complex. *PLoS One* **6,** e28324
38. Jideama, N. M., Crawford, B. H., Hussain, A. K., and Raynor, R. L. (2006) Dephosphorylation specificities of protein phosphatase for cardiac troponin I, troponin T, and sites within troponin T. *Int. J. Biol. Sci.* **2,** 1–9
39. Wijnker, P. J., Boknik, P., Gergs, U., Müller, F. U., Neumann, J., dos Remedios, C., Schmitz, W., Sindermann, J. R., Stienen, G. J., van der Velden, J., and Kirchhefer, U. (2011) Protein phosphatase 2A affects myofilament contractility in non-failing but not in failing human myocardium. *J. Muscle Res. Cell Motil.* **32,** 221–233
40. Hamdani, N., Bishu, K. G., von Frieling-Salewsky, M., Redfield, M. M., and Linke, W. A. (2013) Deranged myofilament phosphorylation and function in experimental heart failure with preserved ejection fraction. *Cardiovasc. Res.* **97,** 464–471
41. Chen, P. P., Patel, J. R., Rybakova, I. N., Walker, J. W., and Moss, R. L. (2010) Protein kinase A-induced myofilament desensitization to Ca^{2+} as a result of phosphorylation of cardiac myosin-binding protein C. *J. Gen. Physiol.* **136,** 615–627
42. Cazorla, O., Szilagyi, S., Vignier, N., Salazar, G., Krämer, E., Vassort, G., Carrier, L., and Lacampagne, A. (2006) Length and protein kinase A modulations of myocytes in cardiac myosin binding protein C-deficient mice. *Cardiovasc. Res.* **69,** 370–380
43. Haj Slimane, Z., Bedioune, I., Lechêne, P., Varin, A., Lefebvre, F., Mateo, P., Domergue-Dupont, V., Dewenter, M., Richter, W., Conti, M., El-Armouche, A., Zhang, J., Fischmeister, R., and Vandecasteele, G. (2014) Control of cytoplasmic and nuclear protein kinase A by phosphodiesterases and phosphatases in cardiac myocytes. *Cardiovasc. Res.* **102,** 97–106
44. Wu, S. C., and Solaro, R. J. (2007) Protein kinase Cζ: a novel regulator of both phosphorylation and de-phosphorylation of cardiac sarcomeric proteins. *J. Biol. Chem.* **282,** 30691–30698
45. Moreno-Gonzalez, A., Korte, F. S., Dai, J., Chen, K., Ho, B., Reinecke, H., Murry, C. E., and Regnier, M. (2009) Cell therapy enhances function of remote non-infarcted myocardium. *J. Mol. Cell Cardiol.* **47,** 603–613
46. Ahn, J.-H., McAvoy, T., Rakhilin, S. V., Nishi, A., Greengard, P., and Nairn, A. C. (2007) Protein kinase A activates protein phosphatase 2A by phosphorylation of the B56δ subunit. *Proc. Natl. Acad. Sci. U.S.A.* **104,** 2979–2984
47. Dodge-Kafka, K. L., Bauman, A., Mayer, N., Henson, E., Heredia, L., Ahn, J., McAvoy, T., Nairn, A. C., and Kapiloff, M. S. (2010) cAMP-stimulated protein phosphatase 2A activity associated with muscle A kinase-anchoring protein (mAKAP) signaling complexes inhibits the phosphorylation and activity of the cAMP-specific phosphodiesterase PDE4D3. *J. Biol. Chem.* **285,** 11078–11086
48. Kho, C., Lee, A., and Hajjar, R. J. (2012) Altered sarcoplasmic reticulum calcium cycling: targets for heart failure therapy. *Nat. Rev. Cardiol.* **9,** 717–733
49. Schwinger, R. H., Münch, G., Bölck, B., Karczewski, P., Krause, E. G., and Erdmann, E. (1999) Reduced Ca^{2+}-sensitivity of SERCA2a in failing human myocardium due to reduced serin-16 phospholamban phosphorylation. *J. Mol. Cell Cardiol.* **31,** 479–491
50. duBell, W. H., Gigena, M. S., Guatimosim, S., Long, X., Lederer, W. J., and Rogers, T. B. (2002) Effects of PP1/PP2A inhibitor calyculin a on the E-C coupling cascade in murine ventricular myocytes. *Am. J. Physiol. Heart Circ. Physiol.* **282,** H38–H48
51. Hall, D. D., Feekes, J. A., Arachchige Don, A. S., Shi, M., Hamid, J., Chen, L., Strack, S., Zamponi, G. W., Horne, M. C., and Hell, J. W. (2006) Binding of protein phosphatase 2A to the L-type calcium channel Cav1.2 next to Ser^{1928}, its main PKA site, is critical for Ser^{1928} dephosphorylation. *Biochemistry* **45,** 3448–3459